Alleviating Bone Cancer–induced Mechanical Hypersensitivity by Inhibiting Neuronal Activity in the Anterior Cingulate Cortex

Chiuan-Shiou Chiou, M.D., Ph.D., Chien-Chung Chen, Ph.D., Tsung-Chih Tsai, B.S., Chiung-Chun Huang, Ph.D., Dylan Chou, B.S., Kuei-Sen Hsu, Ph.D.

ABSTRACT

Background: The anterior cingulate cortex (ACC) is a brain region that has been critically implicated in the processing of pain perception and modulation. While much evidence has pointed to an increased activity of the ACC under chronic pain states, less is known about whether pain can be alleviated by inhibiting ACC neuronal activity.

Methods: The authors used pharmacologic, chemogenetic, and optogenetic approaches in concert with viral tracing technique to address this issue in a mouse model of bone cancer–induced mechanical hypersensitivity by intratibia implantation of osteolytic fibrosarcoma cells.

Results: Bilateral intra-ACC microinjections of γ-aminobutyric acid receptor type A receptor agonist muscimol decreased mechanical hypersensitivity in tumor-bearing mice (n =10). Using adenoviral-mediated expression of engineered $G_{i/o}$-coupled human M4 (hM4Di) receptors, we observed that activation of $G_{i/o}$-coupled human M4 receptors with clozapine-*N*-oxide reduced ACC neuronal activity and mechanical hypersensitivity in tumor-bearing mice (n = 11). In addition, unilateral optogenetic silencing of ACC excitatory neurons with halorhodopsin significantly decreased mechanical hypersensitivity in tumor-bearing mice (n = 4 to 9), and conversely, optogenetic activation of these neurons with channelrhodopsin-2 was sufficient to provoke mechanical hypersensitivity in sham-operated mice (n = 5 to 9). Furthermore, we found that excitatory neurons in the ACC send direct descending projections to the contralateral dorsal horn of the lumbar spinal cord *via* the dorsal corticospinal tract.

Conclusions: The findings of this study indicate that enhanced neuronal activity in the ACC contributes to maintain bone cancer–induced mechanical hypersensitivity and suggest that the ACC may serve as a potential therapeutic target for treating bone cancer pain. **(Anesthesiology 2016; 125:779-92)**

CHRONIC pain is one of the most common medical problems with considerable impact on patient's normal psychologic and physical functions.[1] The prevalence rate of chronic pain is high,[2] but unfortunately, current pain management interventions are still insufficient. The ineffectiveness of current therapeutic strategies is at least partly due to an incomplete understanding of the cellular, molecular, and circuit mechanisms that underlie the development and maintenance of chronic pain.[3–5] While most mechanistic studies in pain research have focused on the dorsal horn of the spinal cord, recent studies have emphasized the importance of the anterior cingulate cortex (ACC) and the insular cortex in the perception and processing of pain.[5–7] Brain imaging studies have shown increased ACC neuronal activity during the presentation of acute noxious stimuli or under chronic pain conditions.[8–10] However, little is known about how painful stimuli activate the ACC and whether the adaptive changes of neuronal activity in the ACC may contribute to the development and maintenance of chronic pain symptoms.

What We Already Know about This Topic

- The anterior cingulate cortex is a brain region associated with many functions including reward, impulse control, and the experience of pain

What This Article Tells Us That Is New

- Using an animal model of bone cancer–induced pain, it was shown that the γ-aminobutyric acid receptor type A agonist muscimol when injected into the anterior cingulate cortex (ACC) could reduce nociceptive sensitization in tumor-bearing mice
- Using optogenetic techniques and engineered receptors to reciprocally regulate the activity of ACC neurons, it was shown that the ACC may regulate nociceptive signaling at the level of the spinal cord

Recent animal studies have highlighted the importance of long-term changes of excitatory synaptic transmission in ACC neurons in maintaining mechanical hypersensitivity.[5,11] For instance, in a mouse model of neuropathic hypersensitivity, it has been found that peripheral nerve injury triggers both long-term presynaptic and postsynaptic

Submitted for publication November 5, 2015. Accepted for publication June 15, 2016. From the Department of Pharmacology, College of Medicine, National Cheng Kung University, Tainan, Taiwan (C.-S.C., T.-C.T., D.C., K.-S.H.); Department of Anesthesiology, China Medical University Hospital, China Medical University, Taichung, Taiwan (C.-S.C.); and Department of Pharmacology, College of Medicine, National Cheng Kung University, Tainan, Taiwan (C.-C.C., T.-C.T., C.-C.H., D.C., K.-S.H.).

 Anesthesiology 2016; 125:779-92

<zdoi;10.1097/ALN.0000000000001237>

enhancement of excitatory synaptic transmission in layer II/III neurons of the ACC.[12] In addition, peripheral inflammation can induce long-term increases in synaptic insertion of α-amino-3-hydroxy-5-methyl-4-isoxazolepropionic acid receptor GluR1 subunits in ACC neurons, which consequently increases the synaptic transmission and exhibits long-lasting mechanical hypersensitivity.[13] More specifically, inhibiting or erasing synaptic potentiation in the ACC effectively alleviates mechanical hypersensitivity in a mouse model of neuropathic pain.[14] In accordance with synaptic studies, we have recently demonstrated that the development and maintenance of bone cancer–induced mechanical hypersensitivity is associated with a functional loss of long-term depression in rostral ACC neurons.[15]

Bone cancer pain is a complex pain state with overlapping but distinct features of both inflammatory and neuropathic pain.[16,17] Cingulotomy has been performed with success (more than 50%) for the treatment of intractable cancer pain.[18,19] Somewhat surprisingly, to date no previous preclinical studies of bone cancer pain have manipulated ACC neuronal activity, leaving untested the hypothesis that bone cancer pain can be alleviated by inhibiting ACC neuronal activity. We hypothesized that pain can be alleviated by inhibiting ACC neuronal activity. To address this hypothesis, we employed integrative pharmacologic, chemogenetic, and optogenetic approaches to reexamine the role of ACC neuronal activity in mechanical sensitivity regulation in a mouse model of bone cancer pain. Our results provide strong evidence that silencing of ACC excitatory neurons can effectively attenuate bone cancer–induced mechanical hypersensitivity and spontaneous flinching.

Materials and Methods

Experimental Animals

All animal procedures described were executed in accordance with the National Institutes of Health Guide for the Care and Use of Laboratory Animals and were approved by the Institutional Animal Care and Use Committee of National Cheng Kung University, Tainan, Taiwan. All experiments were performed with adult (6 to 10 weeks old) male C3H/HeN mice bred in the Laboratory Animal Center of National Cheng Kung University. The strain of C3H/HeN was chosen for its histocompatibility with the National Collection of Type Cultures (NCTC; Public Health England, United Kingdom) clone 2472 fibrosarcoma cells.[15] Mice were housed in groups of four per cage in a temperature- (25° ± 1°C) and humidity-controlled room under a 12:12-h reversed light/dark cycle (lights on 6:00 AM to 6:00 PM) with access to food and water *ad libitum*. The animals were randomly assigned to treatment groups, and experiments were performed in blind manner. The animals were humanely killed by intraperitoneal injection of sodium pentobarbital (100 mg/kg) after completion of the experiments.

Cell Culture and Implantation

NCTC clone 2472 fibrosarcoma cells were obtained from the American Type Culture Collection (USA) and cultured in NCTC 135 medium (Sigma-Aldrich, USA) containing 10% horse serum (Life Technologies, Carlsbad, CA, USA). When cells were preconfluent, they were detached by treatment with trypsin/EDTA (0.05%/0.02%) and then centrifuged at 400*g* for 3 min. The cell pellet was resuspended in phosphate-buffered saline (PBS) and used for implantation.

Implantation of fibrosarcoma cells was performed as previously described.[15,20] Briefly, the mice were anaesthetized with isoflurane (1 to 1.5% in 100% oxygen), and a minimal skin incision was made in the left leg exposing the tibial plateau. A hole was drilled into the medullary cavity with a 27-gauge needle, and 10 μl PBS containing 2×10^5 fibrosarcoma cells were injected with a 29-gauge needle adapted to a Hamilton syringe. To prevent leakage of cells outside the bone, the injection site was closed with tissue glue and thoroughly irrigated with sterile saline. The wound was then closed with skin sutures. Sham-operated controls underwent an identical procedure with the exception that PBS alone was injected.

Nociceptive Testing

Mechanical sensitivity was assessed by von Frey filaments (Semmes-Weinstein monofilaments; Stoelting, USA) during the light cycle between 9:00 AM and 5:00 PM. In the test, the mice were placed on a wire mesh platform, covered with transparent plastic containers, and allowed to acclimatize to their surroundings for at least 1 h. The hind paw was pressed with one of a series of von Frey filaments with logarithmically incremental stiffness (0.16, 0.4, 0.6, 1.0, 1.4, and 2.0 g), presented perpendicular to the plantar surface. Each filament was applied for 2 to 3 s, and a brisk paw withdrawal was taken as positive response. The 50% paw withdrawal threshold was calculated using the traditional Dixon's up-down method as described previously.[21] We considered the appearance of any of the following behavioral characteristics as a withdrawal response: (1) rapid flinch or withdrawal of the paw, (2) spreading of the toes, or (3) immediate licking of the paw according to the description by Iyer *et al.*[22] The behavioral performance was scored by a trained observer blind to the experimental conditions.

Spontaneous Flinching

Mice were placed in a plexiglass chamber with a wire mesh grid floor and allowed to acclimate to the chamber for 30 min. Flinching behavior was measured during a 3-min observation period as described previously.[23] The number of flinches was counted.

Viral Vectors

DNA plasmids encoding plasmid adeno–associated virus (pAAV)-calcium/calmodulin–dependent protein kinase II α (CaMKIIα)–humanized channelrhodopsin 2 (hChR2)

(H134R)-mCherry (Addgene plasmid 26975), pAAV-CaMKIIα-hChR2 (H134R)–enhanced yellow fluorescent protein (eYFP) (Addgene plasmid 26969), pAAV-CaMKIIα–enhanced *Natronomonas pharaonis* halorhodopsin (NpHR) 3.0-eYFP (Addgene plasmid 26971), and pAAV-CaMKIIα-$G_{i/o}$–coupled human M4 (hM4Di)-mCherry (Addgene plasmid 50477) were obtained from Addgene (USA). DNA plasmids encoding pAAV-CaMKIIα-mCherry (#VB1947) and pAAV-CaMKIIα-eYFP (#VB1941) were purchased from Vector Biolabs (USA). Plasmid DNA was amplified, purified, and collected using a standard plasmid maxiprep kit (Qiagen, USA). The purified plasmids were mixed into calcium chloride solution with the DNA plasmid coding adeno-associated virus (AAV) capsid DJ serotype (AAV-DJ) and cotransfected into HEK293T cells using calcium phosphate precipitation methods. Transfected cells were harvested at 72 h after transfection, and the virus was purified using the AAV purification mega kit (Cell Biolabs, Inc., USA). Viral titers were 5×10^{12} particles per milliliters and stored in aliquots at −80°C until use.

Stereotaxic Cannula Implantation and Intracranial Viral Injections

The mice were bilaterally implanted under deep pentobarbital (50 mg/kg, intraperitoneally) anesthesia with 26-gauge stainless steel guide cannulas (Plastics One, USA) in the ACC. The ACC coordinates were +0.2 mm anterior to bregma, ±0.5 mm bilateral to midline, and 1.4 mm ventral to brain surface according to the description by Franklin and Paxinos.[24] The cannulas were fixed to the skull with anchoring screws and acrylic cement. Finally, protective screw-on dust caps were secured on the guide cannulas. The mice were kept on a thermostat-adjusted heating pad throughout the entire surgical procedures and were brought back to their home cages after they became alert and responsive. The mice were allowed to recover for 5 to 7 days before starting the experiments. For *in vivo* optical stimulation, mice were implanted with unilateral optical fibers targeted directly above each viral-transfected ACC at 5 days before starting the behavioral experiments. Doric patchcord optical fibers (NA 0.37; 200-μm core diameter with optimum length; Doric Lenses, Canada) with ferrule connectors were inserted into the guide cannula and secured with acrylic cement. For muscimol inactivation experiments, mice were freely moving and received microinfusion of either PBS (0.5 μl) or muscimol (50 ng in 0.5 μl of PBS; Sigma-Aldrich) through an inner cannula (34 gauge) in each side during a period of 3 min using a 1-μl Hamilton syringe connected to an infusion pump (Model KDS-310, Muromachi Kikai Company, Japan). The infusion cannulas were left in place for an additional 5 min to minimize backflow of the injectant. After the infusion and a 30-min resting period in the behavioral assay platform, mechanical sensitivity was examined. Dose of muscimol was selected on the basis of published studies[25] and pilot experiments in our laboratory. At the end of the behavioral tests, mice were sacrificed by perfusion, and the injection sites were evaluated for each animal.

For intracranial viral injections, mice were anesthetized with 50 mg/kg pentobarbital and then placed into a stereotaxic frame. The mice were unilaterally injected with a total of 0.5 μl of concentrated viral construct solution into the ACC at a rate of 0.1 μl/min by using a 0.5-μl Hamilton syringe with a 34-gauge blunted-tip needle. After the injection, the needles were left in place for an additional 5 min before it was slowly withdrawn to minimize spread of viral particles along the injection tract. After completing injections, the incision was closed using vicryl suture, and mice were returned to their home cages for 1 to 2 weeks until further manipulation. All viral injection sites were verified histologically.

Optical Stimulation

For *in vivo* optical stimulation, the fiber was connected to a 473- or 589-nm, diode-pumped solid-state laser (Laserglow Technologies, Canada) through a fiber optic/physical contact adapter. Laser output was controlled using a Grass S48 stimulator (USA) to deliver light trains at 10 Hz, 10-ms pulse width for 473-nm blue light, and constant light for 589-nm yellow light experiments. Power output was determined using a PM100A power meter coupled to a S130C photodiode sensor (Thorlabs, USA) and analyzed using LabVIEW 8.5 software (National Instruments, USA). The estimated light intensities were 5 mW/mm^2 for blue light stimulation and 8 mW/mm^2 for yellow light stimulation, respectively, which were calculated using a model predicting irradiance in mammalian tissues (http://www.stanford.edu/group/dlab/cgi-bin/graph/chart.php).

Calibrated von Frey filaments were used to assess mechanical sensitivity as described in the nociceptive testing section. In the test, the mice were allowed to acclimate to the testing environment for at least 1 h. We measured withdrawal threshold to mechanical stimuli during an 80-min session consisting of a baseline 20-min light-off epoch, followed by two epochs of 10-min light-on epochs separated by a 20-min light-off epoch, and ending with another 20-min light-off epoch. The mice expressing NpHR in the ACC were unilaterally illuminated using a yellow laser. The mice expressing ChR2 in the ACC were unilaterally illuminated using a blue laser. After behavioral tests, mice were sacrificed by perfusion, and the optical fiber positions were verified for each animal. Only those mice that had accurate optical fiber positions were chosen for analysis.

Chemogenetic Manipulations

For chemogenetic manipulation of ACC excitatory neurons, mice were bilaterally injected with pAAV-CaMKIIα-hM4Di-mCherry into the ACC. Three to four weeks later, mice were injected intraperitoneally with vehicle or clozapine-*N*-oxide (CNO; 10 mg/kg in 5% dimethyl sulfoxide; Sigma-Aldrich) 30 min before the assessment of mechanical sensitivity. For

intra-ACC trials, mice were freely moving and received bilateral microinfusion of either PBS (0.5 μl) or CNO (3μM in PBS, 0.5 μl) through an inner cannula in each side during a period of 3 min. Dose of CNO was selected on the basis of published studies.[26] Mechanical thresholds were measured by von Frey filaments before and at various time points after systemic (0.5, 1, 2, 6, 21, 22, and 25 h) or intra-ACC (1, 20, and 25 h) CNO injections.

Slice Preparation and Patch Clamp Electrophysiology

Slice preparation and whole cell patch clamp recordings were conducted as reported previously.[15] In brief, mice were anesthetized with isoflurane and decapitated, and brains were rapidly removed and placed in ice-cold sucrose artificial cerebrospinal fluid (ACSF) cutting solution (containing [in millimolar]: sucrose, 234; KCl, 2.5; $CaCl_2$, 0.5; $MgCl_2$, 7; $NaHCO_3$, 25; NaH_2PO_4, 1.25; and glucose, 11 at pH 7.3 to 7.4; and equilibrated with 95% O_2–5% CO_2). The coronal slices (270 μm thick) containing the ACC were prepared using a vibrating microtome (VT1200S; Leica, Germany) and transferred to a holding chamber of normal ACSF (containing [in millimolar]: NaCl, 117; KCl, 4.7; $CaCl_2$, 2.5; $MgCl_2$, 1.2; $NaHCO_3$, 25; NaH_2PO_4, 1.2; and glucose, 11 at pH 7.3 to 7.4; and equilibrated with 95% O_2–5% CO_2) and maintained at room temperature for at least 1 h before use.

During recording, slices were placed in a recording chamber of standard design and fixed at the glass bottom of the chamber with a nylon grid on a platinum frame. The chamber consisted of a circular well of low volume (1 to 2 ml) and was perfused constantly at 32.0° ± 0.5°C at a rate of 2 to 3 ml/min. Whole cell recordings were made using a patch clamp amplifier (Axopatch 200B; Axon Instruments, USA) under infrared-differential interference contrast microscope. The patch electrode (3 to 5 MΩ) were backfilled with internal solution (containing [in mM]: K gluconate, 115; KCl, 20; $MgCl_2$, 2; HEPES, 10; EGTA, 0.5; Na_2ATP, 3; Na_3GTP, 0.3; phosphocreatine, 10; pH 7.2; and 280 to 295 mOsm]. Electrical signals were low-pass filtered at 2 kHz and digitized at 10 kHz using a 12-bit analog-to-digital converter (Digidata 1440, Molecular Devices, USA). An Intel Pentium–based computer (ASUS G20CB, Taiwan) with pCLAMP software (version 9.0; Molecular Devices) was used for on-line acquisition and off-line analysis of the data. For current clamp experiments to confirm the expression of hM4Di in ACC neurons, a depolarizing current pulses (200 pA, 1 s) was injected into the $hM4Di^-$ (no hM4Di expression) and $hM4Di^+$ (hM4Di expression) neurons to induce spiking. After 10 min of continuous recordings, CNO (1 μM) was applied into the ACSF and a second depolarizing current pulse (200 pA, 1 s) was injected into the $hM4Di^-$ and $hM4Di^+$ neurons to induce spiking in order to compare spiking before and after CNO application.

For *in vitro* optical stimulation, a multimode optic fiber (200-μm diameter; Thorlabs), coupled to a diode-pumped solid-state laser of specific wavelength (473 nm blue and 589 nm yellow laser; Laserglow Technologies), was used. Peak and steady-state photocurrents were measured from a 1-s light pulse in voltage clamp mode, where cells were held at −65 mV. For current clamp experiments to characterize the spiking fidelity of ChR2-expressing ACC neurons, optical stimulation (473 nm) was applied at 10 Hz with 10 mW/mm^2. For the NpHR-expressing ACC neuron spiking inhibition experiments, neurons were held at −50 mV to elicit spontaneous activity in current clamp mode, and illumination with yellow light (589 nm) was applied to inhibit spike firing at 10 Hz for 1 s with 10 mW/mm^2.

Immunofluorescence

The mice were deeply anesthetized with sodium pentobarbital (50 mg/kg, intraperitoneally) and perfused transcardially with PBS and 4% paraformaldehyde. After the perfusion, brains and spinal cords were removed and further fixed in 4% paraformaldehyde for 24 h at 4°C and then transferred to the solution containing 30% sucrose that immersed in 4°C for at least 48 h before slicing. Coronal slices were sectioned to a 40-μm thickness, washed with 0.3% Triton X-100, and then incubated for blocking with solution containing 3% goat serum in PBS. After blocking, the sections were incubated in the primary antibodies against c-Fos (1:2,000, rabbit polyclonal IgG; Santa Cruz Biotechnology, USA), mCherry (1:2,000; rabbit polyclonal IgG; Abcam, USA), GFP (1:2,000, rabbit polyclonal IgG; Abcam), or neuronal nuclei (NeuN, 1:2,000, mouse monoclonal IgG; Merck Millipore, USA) overnight at 4°C in blocking buffer with 0.1% Triton X-100. Finally, sections were washed with Tris-buffered saline and Tween 20 (TBS-T; 10 mM, Tris–HCl, 150 mM NaCl, and 0.025% Tween 20; pH 7.4) and then incubated with the secondary Alexa Fluor 488 or Alexa Fluor 594 antibodies (Life Technologies, Grand island, NY, USA) for 2 h at room temperature in blocking buffer. The immunostained sections were collected on separate gelatin-subbed glass slides, rinsed extensively in PBS, and mounted with ProLong Gold Antifade Reagent (Invitrogen, USA). Fluorescence microscopic images of neurons were obtained using an Olympus BX51 microscope coupled to an Olympus DP70 digital camera (Olympus, Japan) or a FluoView1000 confocal microscope (Olympus) with sequential acquisition setting at a resolution of 680 × 680 pixels, z-stack with 15 to 20 optical sections. All images were imported into ImageJ software (NIH, USA) for analysis, and all the parameters used were kept consistent during capturing. The fluorescence intensity of c-Fos was measured with ImageJ software (NIH) as described previously.[27] For analysis, serial coronal sections located −0.1 to 1.34 mm from bregma were selected. All optical parameters were kept constant throughout all measurements. Regions of ACC were sampled randomly to avoid sampling bias. All counting was performed in a blind manner.

Virus Anterograde Tracing

The mice were unilaterally injected with a total of 0.5 μl of pAAV-CaMKIIα-hM4Di-mCherry into the ACC. Four weeks after infection, mice were deeply anesthetized with sodium pentobarbital (50 mg/kg, intraperitoneally) and perfused transcardially with PBS and 4% paraformaldehyde. Coronal brain slices containing the ACC and transverse spinal slices containing both cervical and lumbar enlargements were sectioned to a 40-μm thickness. The sections were incubated in the primary antibodies against mCherry (1:2,000; Abcam) and neuronal nuclei (NeuN, 1:2000; Merck Millipore) overnight at 4°C in PBS with 0.1% Triton X-100. Finally, sections were washed with TBS-T and then incubated with the secondary anti-mouse Alexa Fluor 488 and anti-rabbit Alexa Fluor 594 antibodies (Life Technologies, Grand island, NY, USA) for 2 h at room temperature. The immunostained sections were collected on separate gelatin-subbed glass slides, rinsed extensively in PBS, and mounted with ProLong Gold Antifade Reagent (Invitrogen). Fluorescence microscopic images of neurons were obtained using an Olympus BX51 microscope coupled to an Olympus DP70 digital camera (Olympus).

Statistical Analysis

No statistical methods were used to predetermine sample size, but our sample sizes were based on our previous publication.[15] The data were normally distributed and were expressed as means ± SEM. All statistical analyses were performed using the Prism 6 software package (GraphPad Software, Inc., USA). The significance of any difference between two groups was calculated using the paired or unpaired Student's *t* test. The significance of the difference between multiple groups was calculated by two-way ANOVA followed by Bonferroni *post hoc* analyses. No experimental data were missing or lost to statistical analysis. Number of animals used is indicated by n. Probability values of $P < 0.05$ were considered to represent significant differences.

Results

Microinjection of Muscimol into the ACC Decreased Mechanical Hypersensitivity in Tumor-bearing Mice

To investigate the role of ACC neuronal activity in mechanical sensitivity regulation, we used a mouse model of bone cancer pain induced by intratibia implantation of osteolytic fibrosarcoma cells. Consistent with our previous findings,[15] tumor-bearing mice showed increased sensitivity to mechanical stimuli of the ipsilateral hind paw with normally nonnoxious von Frey filaments on days 9, 12, 15, 18, 21, and 24 postoperation when compared with sham-operated mice. A two-way repeated measure ANOVA of mechanical threshold revealed a significant treatment × time interaction ($F_{(24,394)} = 6.5$, $P < 0.001$), a significant effect of treatment ($F_{(3,394)} = 83.7$, $P < 0.001$), and a significant effect of time ($F_{(8,394)} = 12.9$, $P < 0.001$; fig. 1A). The progressive decrease of mechanical withdrawal threshold on the ipsilateral side of tumor-bearing mice began by postoperative day 9 (1.2 ± 0.2 g, n = 12), which is significantly less than the threshold observed on the contralateral side of tumor-bearing mice (2.4 ± 0.1 g, n = 12) or sham-operated mice (ipsilateral: 2.2 ± 0.2 g, contralateral: 2.2 ± 0.2 g, n = 12), and persisted thereafter throughout the study.

To determine whether ACC neuronal activity regulates mechanical sensitivity, we bilaterally injected γ-aminobutyric acid receptor type A receptor agonist muscimol into the ACC of sham-operated and tumor-bearing mice on day 21 postoperation and then measured the withdrawal threshold to mechanical stimulation (fig. 1B). As shown in figure 1, C and D, microinjection of muscimol into the ACC significantly decreased mechanical hypersensitivity in tumor-bearing mice, as confirmed by a two-way repeated measure ANOVA, a significant treatment × time interaction ($F_{(3,52)} = 3.9$, $P = 0.014$), a significant effect of treatment ($F_{(1,52)} = 27.3$, $P < 0.0001$), and a significant effect of time ($F_{(3,52)} = 4.3$, $P = 0.008$). In contrast, muscimol treatment did not affect the mechanical sensitivity in sham-operated mice.

Chemogenetic Silencing of Excitatory Neurons in the ACC Decreased Mechanical Hypersensitivity and Spontaneous Flinching in Tumor-bearing Mice

One of the main limitations of the conventional pharmacologic approaches is the lack of specificity for the cell types being targeted. To overcome this limitation, we used a chemogenetic approach to selectively and temporarily silence ACC excitatory neurons. We bilaterally injected the ACC with a recombinant AAV-DJ expressing an engineered $G_{i/o}$-coupled receptor hM4Di tagged with a fluorescent protein mCherry (hM4Di-mCherry), under control of the CaMKIIα promoter, favoring expression within excitatory neurons,[28] and then performed intratibia implantation of osteolytic fibrosarcoma cells into mice. Our immunohistochemical analysis indicated that mCherry-expressing cells were positive for CaMKIIα, suggesting that hM4Di is preferentially expressed in excitatory neurons in the ACC (data not shown). The experimental procedure is depicted in figure 2A. At 22 to 28 days after AAV injection, mice were treated with CNO, a synthetic ligand of hM4Di,[29] and then the withdrawal threshold to mechanical stimulation was measured. *Post hoc* histologic examination of brain sections revealed robust and bilateral expression of hM4Di in neurons in the ACC (fig. 2B). In a subset of mice, we performed *ex vivo* electrophysiologic recordings to confirm the effects of CNO in AAV-infected neurons. Application of CNO (1 μM) significantly decreased spiking responses to 200 pA square current pulses in hM4Di-expressing ($hM4Di^+$) neurons (fig. 2C). To ensure that hM4Di/CNO-based approach is functional in the brain, we examined the expression of c-Fos immunoreactivity, a marker for recent neuronal excitation, in the ACC of tumor-bearing mice, both before and after intraperitoneal CNO injection. A significant decrease in the expression of c-Fos immunoreactivity was observed in the ACC followed by intraperitoneal injection of CNO

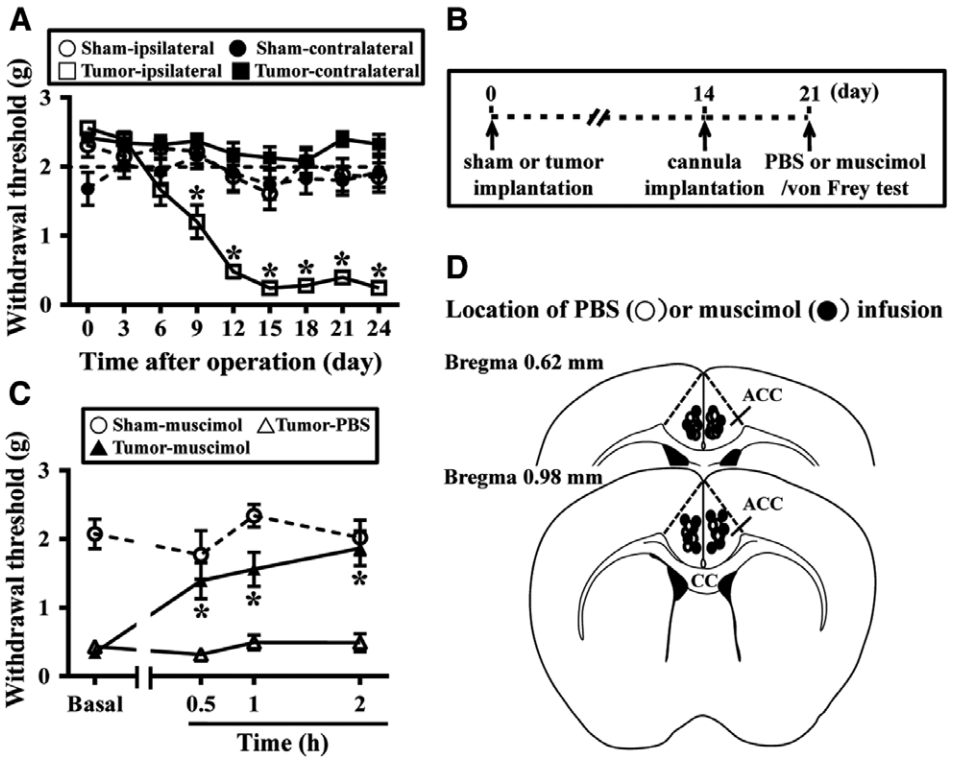

Fig. 1. Bilateral microinjection of muscimol into the anterior cingulate cortex (ACC) decreased mechanical hypersensitivity in tumor-bearing mice. (*A*) The withdrawal threshold to nonnoxious mechanical stimulation with von Frey filament was selectively decreased in the ipsilateral hind paw of tumor-bearing mice (n = 12) compared with sham-operated mice beginning by post-operative day 9 (n = 12). **P* < 0.05 as compared with sham-ipsilateral group by two-way ANOVA with Bonferroni *post hoc* test. (*B*) Schematic representation of the experimental design. Fourteen days after sham or tumor implantation, mice were surgically implanted with bilateral cannulas into the ACC. Mice were allowed 7 days to recover. On day 21, ACC was bilaterally injected with phosphate-buffered saline (PBS, 0.5 μl/side) or muscimol (50 ng/0.5 μl/side) 30 min before the von Frey test. (*C*) Microinjection of muscimol into the ACC significantly reduced mechanical hypersensitivity in tumor-bearing mice (n = 10), compared with the PBS control (n = 5). Muscimol had no discernible effects on paw withdrawal thresholds in sham-operated mice (n = 6). (*D*) Schematic illustration of coronal sections illustrating the microinjection sites in the bilateral ACC. Data are presented as means ± SEM. **P* < 0.05 as compared with tumor–PBS group by two-way ANOVA with Bonferroni *post hoc* test.

(10 mg/kg). The levels of c-Fos immunoreactivity were noted to be decreased at 6 h and returned to basal levels at 22 h after CNO treatment (fig. 2, D and E). In parallel, we found that hM4Di/CNO-based approach, compared with hM4Di/vehicle treatment, significantly decreased mechanical hypersensitivity in tumor-bearing mice, as confirmed by a two-way repeated measure ANOVA, a significant treatment × time interaction ($F_{(7, 187)} = 4.3$, $P < 0.001$), a significant effect of treatment ($F_{(1,187)} = 64.9$, $P < 0.001$), and a significant effect of time ($F_{(7,187)} = 4.5$, $P < 0.001$; fig. 2F). To confirm the specificity of the CNO action, we also injected hM4Di mice with CNO (3 μM, 0.5 μl per side) into the ACC and then test them on mechanical hypersensitivity. Inhibition of the ACC with local CNO microinjection significantly reduced mechanical hypersensitivity in tumor-bearing mice compared to vehicle-treated littermates (fig. 3).

Behavioral analysis of spontaneous flinching was employed to assess the effect of silencing ACC neuronal activity with hM4Di/CNO-based approach. In agreement with previous studies,[23] tumor-bearing mice showed spontaneous flinching behavior on days 12, 15, 18, and 21 postoperation when compared with sham-operated mice. A two-way repeated measure ANOVA of mechanical threshold revealed a significant treatment × time interaction ($F_{(7,64)} = 33.1$, $P < 0.001$), a significant effect of treatment ($F_{(1,64)} = 189.2$, $P < 0.001$), and a significant effect of time ($F_{(7,64)} = 28.1$, $P < 0.001$; fig. 4A). CNO (10 mg/kg) injection significantly decreased flinching behavior in tumor-bearing mice with hM4Di expression in the ACC on day 21 postoperation compared to vehicle-treated littermates ($t_{(18)} = 2.6$, $P = 0.008$; fig. 4B). CNO had no effect in sham-operated mice with hM4Di expression in the ACC.

We also examined the motor function after ACC manipulation. Sham and tumor-bearing mice with hM4Di expression in the ACC on day 21 postoperation displayed comparable levels of locomotor activity, when examined under CNO (10 mg/kg) or vehicle treatment (data not shown).

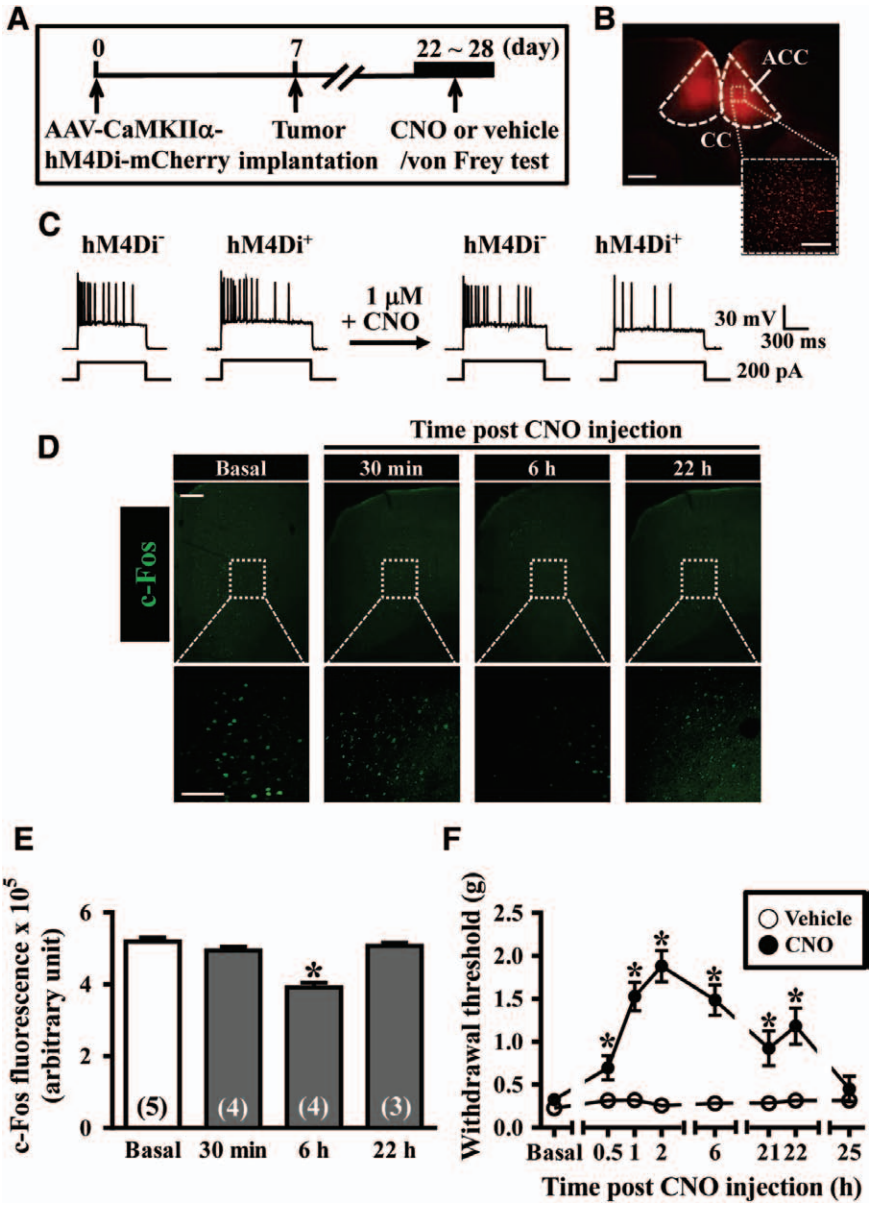

Fig. 2. Activation of $G_{i/o}$–coupled human M4 (hM4Di) receptors with clozapine-*N*-oxide (CNO) in anterior cingulate cortex (ACC) excitatory neurons decreased mechanical hypersensitivity in tumor-bearing mice. (*A*) Schematic representation of the experimental design. Seven days after stereotaxic injection of adeno-associated virus (AAV)–calcium/calmodulin-dependent protein kinase II α (CaMKIIα)-hM4Di-mCherry construct into the ACC, mice were surgically implanted with tumor cells. Fifteen to 21 days later, mice received the systemic agonist CNO (10 mg/kg, intraperitoneal) or vehicle, and paw withdrawal thresholds were determined using von Frey filaments. (*B*) Coronal micrograph showing the expression of hM4Di receptors in the ACC. *Scale bars* represent 500 and 100 μm (rectangle amplification). (*C*) Representative traces showing responses of uninfected (hM4Di⁻)and infected (hM4Di⁺) neurons to depolarizing current pulse (200 pA) under whole cell current clamp before and after bath application of CNO (1 μM) in the *ex vivo* ACC slices. (*D*) Activation of ACC neurons before and after CNO injection assessed by c-Fos immunofluorescence in tumor-bearing mice. *Scale bars* represent 200 and 100 μm (rectangle amplification). (*E*) Quantification of the activation of neurons in the ACC before and after CNO injection. The total number of animals examined is indicated by n in parentheses. Data are presented as means ± SEM. **P* < 0.05 as compared with basal condition by unpaired Student's *t* test. (*F*) Summary of experiments showing the effects of vehicle (n = 7) and CNO injection (n = 11) on paw withdrawal thresholds in tumor-bearing mice that received bilateral injections of AAV-CaMKIIα-hM4Di-mCherry in the ACC. Mechanical thresholds were measured by von Frey filaments before (basal) and at 0.5, 1, 2, 6, 21, 22, and 25 h after systemic CNO injection. **P* < 0.05 as compared with vehicle group by two-way ANOVA with Bonferroni *post hoc* test.

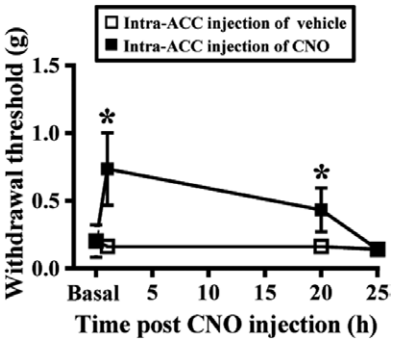

Fig. 3. Summary of experiments showing the effects of intraanterior cingulate cortex (ACC) injection of vehicle (phosphate-buffered saline, 0.5 μl; n = 5) or clozapine-*N*-oxide (CNO; 3 μM in phosphate-buffered saline, 0.5 μl; n = 8) on paw withdrawal thresholds in tumor-bearing mice that received bilateral injections of adeno-associated virus (AAV)–calcium/calmodulin-dependent protein kinase II α-$G_{i/o}$–coupled human M4-mCherry in the ACC. Mechanical thresholds were measured by von Frey filaments before (basal) and at 1, 20, and 25 h after intra-ACC CNO injection. **P* < 0.05 as compared with vehicle group by two-way ANOVA with Bonferroni *post hoc* test.

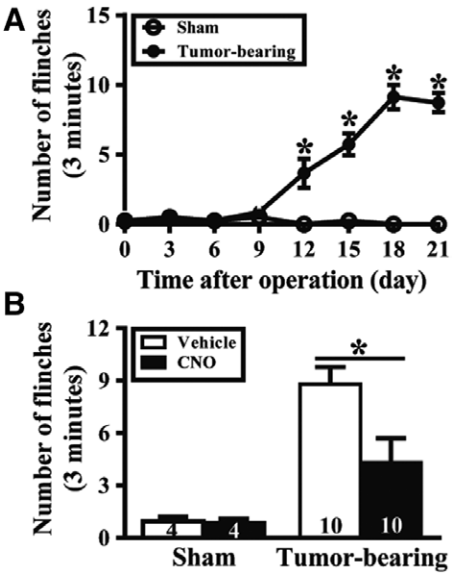

Fig. 4. Activation of $G_{i/o}$–coupled human M4 (hM4Di) receptors with clozapine-*N*-oxide (CNO) in anterior cingulate cortex (ACC) excitatory neurons decreased spontaneous pain-related flinching behavior in tumor-bearing mice. (*A*) The number of flinches was significantly increased in tumor-bearing mice (n = 5) compared with sham-operated mice beginning by postoperative day 12 (n = 5). **P* < 0.05 as compared with sham group by two-way ANOVA with Bonferroni *post hoc* test. (*B*) Summary of experiments showing the effects of vehicle and CNO injection on the number of flinches in sham-operated and tumor-bearing mice with hM4Di expression in the ACC on day 21 postoperation. The total number of animals examined is indicated by n in parentheses. Data are presented as means ± SEM. **P* < 0.05 as compared with vehicle group by unpaired Student's *t* test.

Optogenetic Silencing of Excitatory Neurons in the ACC Decreased Mechanical Hypersensitivity in Tumor-bearing Mice

Given that optogenetics permits bidirectional manipulation of neuronal activity with anatomical, genetic, and temporal precision, we also used *in vivo* optogenetic approaches to study the role of the ACC in mechanical sensitivity modulation. To evaluate whether optogenetic silencing of excitatory ACC neuronal activity would modulate mechanical sensitivity, we unilaterally injected AAV encoding the light-sensitive chloride pump, NpHR (AAV-CaMKIIα-NpHR-eYFP; referred to as NpHR), or AAV-CaMKIIα-eYFP as a control into the ACC of tumor-bearing mice. The experimental procedure is depicted in figure 5A. Three weeks later, mice received photostimulation and the withdrawal threshold to mechanical stimulation was measured. *Post hoc* histologic examination of brain sections revealed robust and unilateral expression of NpHR in neurons in the ACC (fig. 5B). Functional validation of AAV-infected neurons using *ex vivo* whole cell patch clamp recordings confirmed that constant yellow light illumination (589 nm) reliably elicited a strong hyperpolarization and reversibly abolished spontaneous spike firing in slices from NpHR-injected mice (fig. 5C). *In vivo*, we observed that light illumination of either the ipsilateral or contralateral ACC significantly produced an acute and rapid decrease in mechanical hypersensitivity in NpHR-expressing tumor-bearing mice (fig. 5D). In contrast, there was no effect of light illumination in eYFP-injected, control tumor-bearing mice. The effect of light illumination was fully reversible and repeatable. The withdrawal thresholds to mechanical stimulation were significantly higher at the light-on epochs (ipsilateral: 0.71 ± 0.12 g, n = 7; contralateral: 0.74 ± 0.11 g, n = 9, $P < 0.001$) than at the light-off epoch (ipsilateral: 0.25 ± 0.12 g, n = 7; contralateral: 0.28 ± 0.05 g, n = 9; fig. 5D) in NpHR-injected tumor-bearing mice.

Optogenetic Activation of Excitatory Neurons in the ACC Provokes Mechanical Hypersensitivity in Sham-operated Mice

As the ablation of ACC excitatory neuronal activity decreased mechanical hypersensitivity in tumor-bearing mice, we wondered whether activation of these neurons could elicit mechanical hypersensitivity. To address this question, we unilaterally injected AAV encoding the light-sensitive channelrhodopsin-2 (AAV-CaMKIIα-hChR2 (H134R)-mCherry; referred to as ChR2), or AAV-CaMKIIα-mCherry as a control, into the ACC of sham-operated mice. The experimental procedure is depicted in figure 6A. Three weeks later, mice received photostimulation and the withdrawal threshold to mechanical stimulation was measured. *Post hoc* histologic examination of brain sections revealed robust and unilateral expression of ChR2 in the ACC neurons (fig. 6B). Functional validation of AAV-infected neurons using *ex vivo* whole cell patch clamp recordings confirmed that blue light illumination (473 nm) reliably

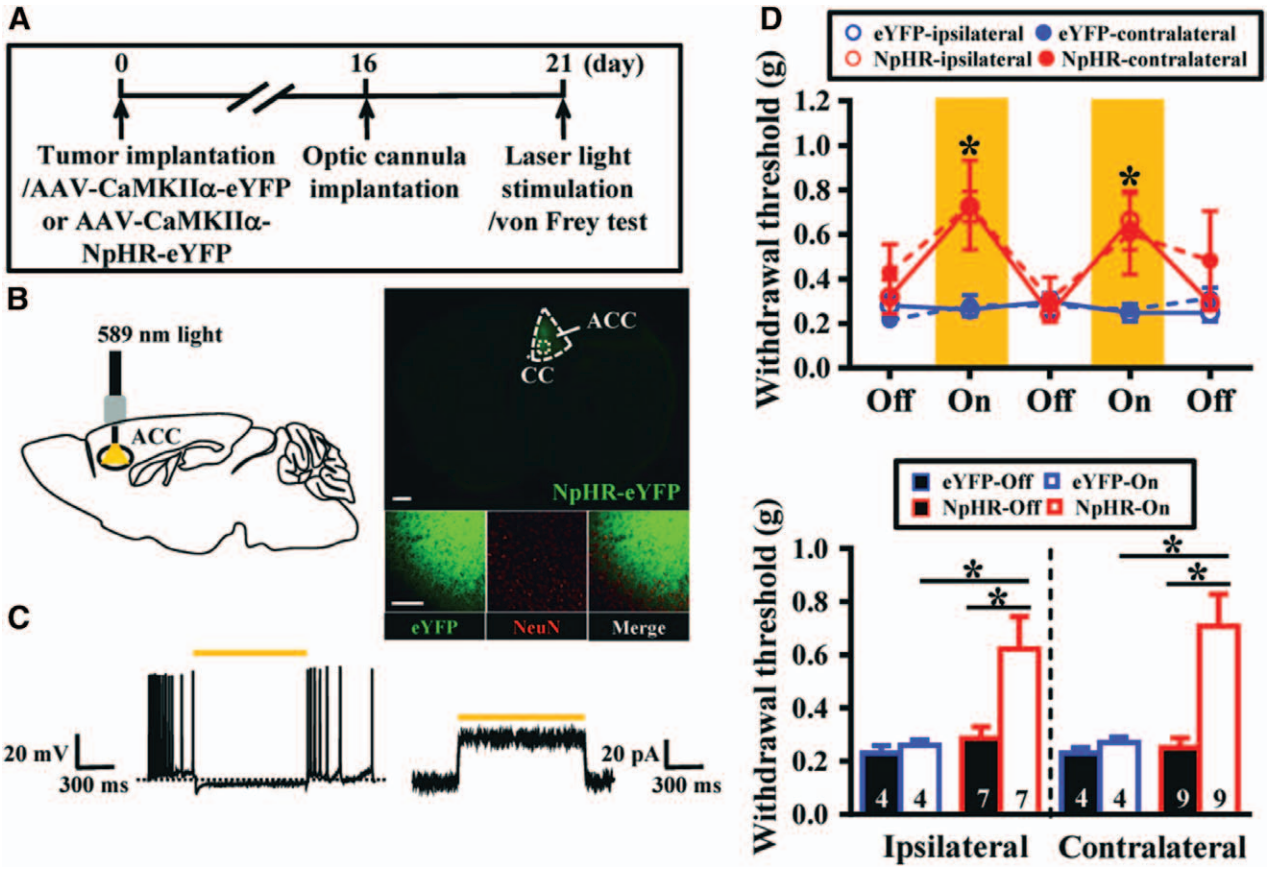

Fig. 5. Natronomonas *pharaonis* halorhodopsin (NpHR) silencing of anterior cingulate cortex (ACC) excitatory neurons decreased mechanical hypersensitivity in tumor-bearing mice. (*A*) Schematic representation of the experimental design. Sixteen days after tumor implantation and stereotaxic injection of adeno-associated virus (AAV)–calcium/calmodulin-dependent protein kinase II α (CaMKIIα)-enhanced yellow fluorescent protein (eYFP) or AAV-CaMKIIα-NpHR-eYFP construct into the ACC, mice were surgically implanted with unilateral cannulas into the virus-infected ACC, either ipsilateral or contralateral to the tumor-bearing leg. Five days later, mice received light treatment in the ACC, and paw withdrawal thresholds were determined using von Frey filaments. (*B*) *Left*, Schematic drawing showing the yellow light (589 nm) treatment. *Right*, Coronal micrograph showing the expression of NpHR in the ACC. *Scale bars* represent 2 nm and 200 μm (rectangle amplification). (*C*) *Left*, Representative whole cell current clamp recording showing yellow light (589 nm)–mediated inhibition of spontaneous spike firing in NpHR-expressing ACC neurons held at −50 mV. *Right*, Representative whole cell voltage clamp recording showing outward photocurrent in an NpHR-expressing ACC neuron exposed to a 1-s, 589-nm light pulse. (*D*) Photoinactivation of ACC neurons decreased mechanical hypersensitivity in tumor-bearing mice expressing NpHR or eYFP (*top*). Ipsilateral and contralateral refer to the side of the paw tested. Summary graph showing the average of different withdrawal threshold values in each epoch (*bottom*). The total number of animals examined is indicated by n in parentheses. Data are presented as means ± SEM. *$P < 0.05$ as compared with light-off condition or eYFP-on group by paired or unpaired Student's *t* test.

elicited action potentials and strong inward currents in slices from ChR2-injected mice (fig. 6C). *In vivo*, we observed that light illumination of either the ipsilateral or contralateral ACC significantly produced an acute and reproducible fall in the withdrawal threshold to mechanical stimulation in sham-operated mice (fig. 6D). In contrast, there was no effect of light illumination in mCherry-injected control sham-operated mice. The effect of light illumination was fully reversible and repeatable. The withdrawal thresholds to mechanical stimulation were significantly lower at the light-on epochs (ipsilateral: 1.49 ± 0.13 g, n = 9; contralateral: 1.22 ± 0.13 g, n = 5, $P < 0.01$) than at the light-off epochs (ipsilateral: 2.06 ± 0.11 g, n = 9; contralateral: 2.01 ± 0.12 g, n = 5; fig. 6D) in ChR2-injected sham-operated mice. Furthermore, we found a significant increase in the number of cells colabeled for c-Fos and ChR2-eYFP in response to light illumination in the ACC when compared with light illumination in mice expressing eYFP alone (data not shown).

Corticospinal Projections from the ACC to the Spinal Cord Dorsal Horn

Given that the spinal cord dorsal horn is important for the transmission of nociceptive information, we next asked whether ACC excitatory neurons may send their projecting fibers directly to the spinal cord dorsal horn in adult C3H/HeN mice. Taking advantage of the anterograde transport

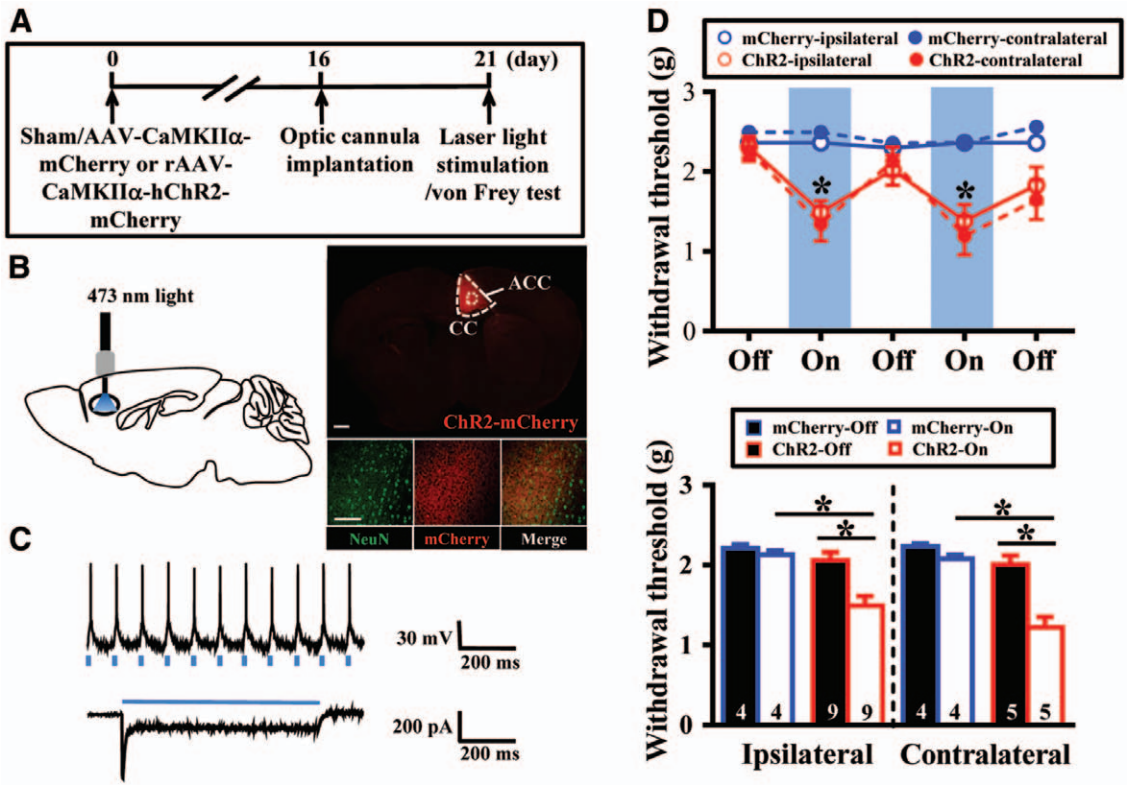

Fig. 6. Channelrhodopsin-2 (ChR2) activation of anterior cingulate cortex (ACC) neurons reduced paw withdrawal thresholds in sham-operated mice. (*A*) Schematic representation of the experimental design. Sixteen days after sham operation and stereotaxic injection of adeno-associated virus (AAV)–calcium/calmodulin-dependent protein kinase II α (CaMKIIα)-mCherry or AAV-CaMKIIα-ChR2-mCherry construct into the ACC, mice were surgically implanted with unilateral cannulas into the virus-infected ACC, either ipsilateral or contralateral to the sham-operated leg. Five days later, mice received light treatment in the ACC, and paw withdrawal thresholds were determined using von Frey filaments. (*B*) *Left*, Schematic drawing showing the blue light (473 nm) treatment. *Right*, Coronal micrograph showing the expression of ChR2 in the ACC. *Scale bars* represent 2 nm and 200 μm (*rectangle* amplification). (*C*) *Top*, Representative whole cell current clamp recording showing action potentials induced by 473-nm light in ChR2-expressing ACC neurons. *Bottom*, Representative whole cell voltage clamp recording showing inward photocurrent in a ChR2-expressing ACC neuron exposed to a 1-s, 473-nm light pulse, at a holding potential of −65 mV. (*D*) Photoactivation of ACC neurons decreased paw withdrawal thresholds in sham-operated mice expressing ChR2 or mCherry (*top*). Ipsilateral and contralateral refer to the side of the paw tested. Summary graph showing the average of different withdrawal threshold values in each epoch (*bottom*). The total number of animals examined is indicated by n in parentheses. Data are presented as means ± SEM. **P* < 0.05 as compared with light-off condition or mCherry-on group by paired or unpaired Student's *t* test.

capability of AAV vector, mCherry expression allowed us to identify the transduced ACC efferent toward their destinations. We found that, 4 weeks after infection of AAV-CaMKIIα-hM4Di-mCherry into the ACC, the expression of mCherry was readily detected in the ACC and the spinal cord of naive mice. In the ipsilateral ACC, mCherry expression was found to be commonly colocalized with the neuronal marker NeuN (fig.7A). Consistent with recent findings,[30] mCherry-expressing fibers were detected in the contralateral dorsal horn laminae I to II and III to V of the lumbar section of the spinal cord *via* the dorsal corticospinal tract (fig. 7B).

Discussion

In this study, we have demonstrated for the first time that direct manipulation of ACC neuronal activity can dramatically alter mechanical sensitivity in a mouse model of bone cancer pain. Particularly, silencing ACC excitatory neurons produced a significant decrease in bone cancer–induced mechanical hypersensitivity and spontaneous flinching. Conversely, optogenetic activation of excitatory neurons in the ACC provokes mechanical hypersensitivity in sham-operated mice. Consistent with previous anterograde and retrograde tracing studies,[30] we have confirmed the existence of a direct descending projection from the ACC to the contralateral dorsal horn of the lumbar spinal cord *via* the dorsal corticospinal tract. Together, these data provide experimental support for the concept that the ACC contributes to pain perception and its modulation.

Human brain imaging and animal studies have shown that the ACC undergoes structural and functional changes with chronic pain and long-lasting mechanical

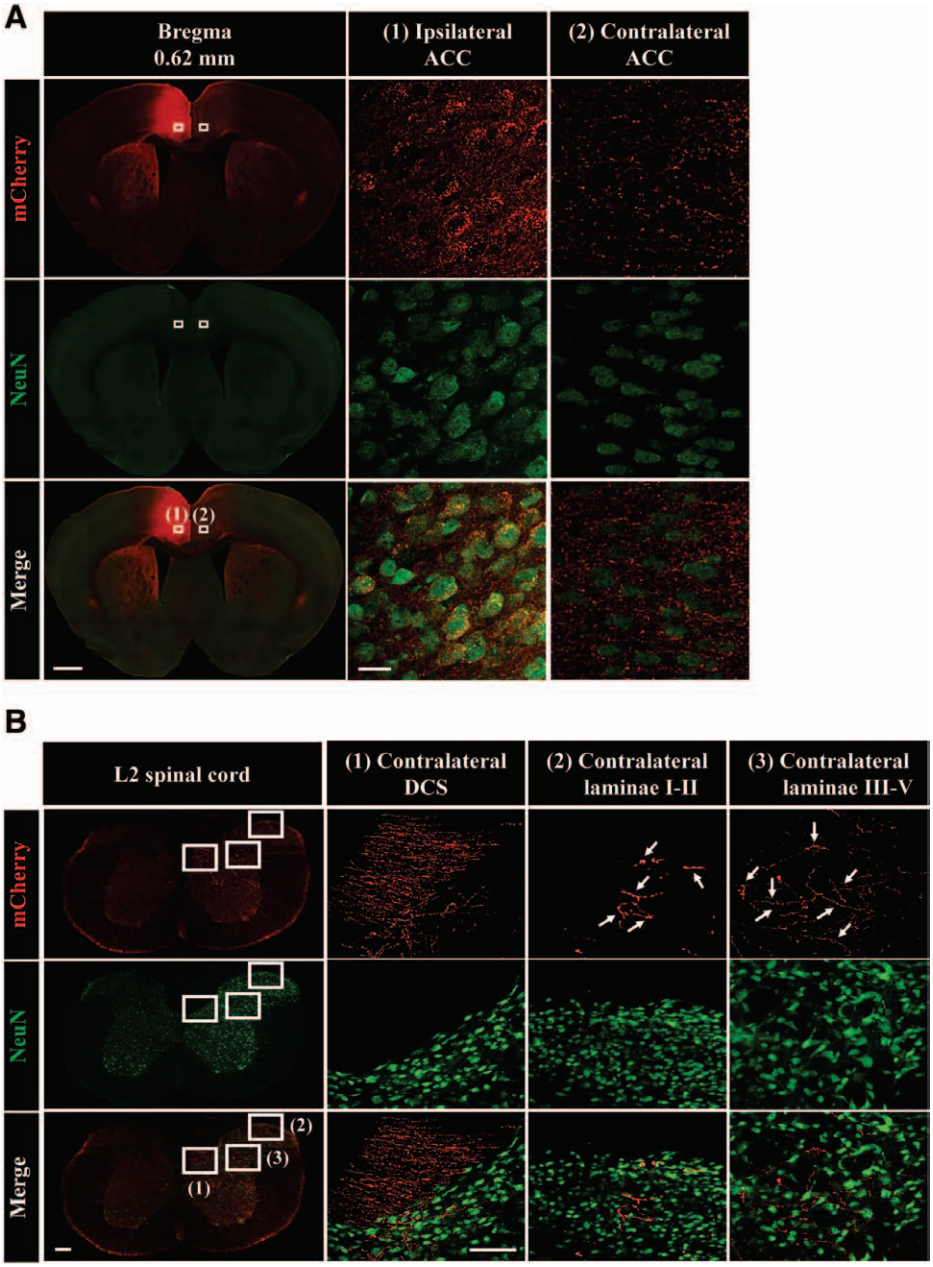

Fig. 7. Distribution of adeno-associated virus anterograde mCherry labeling of fibers in the spinal dorsal horn projected from the anterior cingulate cortex (ACC). (*A*) *Left*, Representative images showing the distribution of mCherry labeling of fibers in the ipsilateral and the contralateral ACC to the virus injection (bregma 0.62 mm). *Middle* and *right*, Augmented figures showing mCherry and NeuN double-labeling results in *rectangle areas* (1) and (2). *Scale bars*: *Left*, 2 mm; *middle*, 50 μm. (*B*) *Left*, Representative images showing the distribution of mCherry labeling of fibers in the dorsal horn laminae I to II and III to V of the lumbar section of the spinal cord projected from the ACC. *Rectangle areas* of (1) to (3) were augmented in the *right*, respectively. *Arrows* denote mCherry-expressing projected fibers from the ACC. (1) Contralateral dorsal corticospinal (DCS) tract; (2) contralateral laminae I to II; (3) contralateral laminae III to V. *Scale bars*: *Left*, 0.5 mm; *middle*, 100 μm.

hypersensitivity.[5,8–15,31] Conceptually, pain comprises both sensory and affective components. The sensory component is commonly represented by rating of pain intensity and quality, whereas the affective component is represented by rating of pain unpleasantness.[7] There is some evidence supporting the notion that the sensory and affective components of pain are processed by partially dissociable brain networks. Clinical imaging studies have shown that somatosensory cortical neuronal activity is correlated with the intensity of the noxious stimulus, whereas ACC neuronal activity is correlated with subjective unpleasantness,[32,33] suggesting a differentially functional requirement for the somatosensory cortex and the ACC in pain perception.[34] Some animal behavioral studies using the formalin-induced

conditioned place avoidance or place escape/avoidance paradigm also supported the hypothesized involvement of the ACC in mediating the affective-like responses.[35–37] In addition, a recent study has reported a significant association of the ACC with the anxiodepressive consequences in a mouse model of neuropathic pain.[38] It is noteworthy that although these studies strongly support a role for the ACC in encoding the affective component, some animal studies have suggested an involvement of the ACC in the sensory component. For example, pharmacologic studies have revealed that inhibiting or erasing nerve injury– or inflammation-induced synaptic potentiation in the ACC can effectively reduce mechanical hypersensitivity.[14,39] These findings may contrast with previous reports showing that electrolytic lesions of the ACC selectively decreased formalin-induced inflammatory nociceptive responses but had no effect on enhanced mechanical paw withdrawal thresholds in the neuropathic nociceptive model.[40] Our previous studies have demonstrated that the increase of ACC neuronal activity is correlated with the development of mechanical hypersensitivity in tumor-bearing mice.[15] In the current study, by applying optogenetic and chemogenetic silencing of excitatory neurons in the ACC, we confirm that enhanced ACC neuronal activity may contribute to the expression of mechanical hypersensitivity in tumor-bearing mice. This notion is further supported by using the optogenetic approach showing that repeated activation of excitatory neurons in the ACC provoked decreased withdrawal threshold to mechanical stimulation in sham-operated mice. These observations may thus be supportive of a prominent role for the ACC in the sensory component of the mouse model of bone cancer pain. There are three potential interpretations for these apparently disparate observations. First, it is possible that although the ACC is of particular importance for the perception and evaluation of the affective component, altered ACC activity may modulate neural circuitry mediating sensory component. This interpretation is supported by our and other laboratory's results showing that some of ACC excitatory neurons send direct descending projecting fibers to laminae III to V of the spinal cord dorsal horn.[30] Second, the neural subtracts underlying the affective component may not be completely dissociated from the neural subtracts encoding its sensory component. Third, it is also possible that von Frey filament–based assessment of rodent mechanical sensory threshold may partially recruit certain items related to the affective component. Further studies will be required to examine these possibilities. Our data are in agreement with previous clinical observations demonstrating that surgical cingulotomy/capsulotomy resulted in an increased heat pain threshold and increased rating to suprathreshold noxious heat stimuli, suggesting a role for the ACC in the modulation of pain sensation.[41]

It is worth noting, however, that the reversion on bone cancer–induced mechanical hypersensitivity after stimulation with yellow light illumination seems quite moderate compared to one obtained after intraperitoneal injection of CNO. The reasons for this are unclear but may be related to differences in mechanism of action or efficacy between optogenetic and chemogenetic approaches. Indeed, virally mediated optogenetic inhibition of pain can be directly achieved by fast-acting membrane potential stabilization, whereas chemogenetic stimulations involve second messenger activation and altered pattern of gene expression.[42] Because local microinjections of CNO into the ACC mimicked the effect of systemic administration of CNO in reducing mechanical hypersensitivity in hM4Di-expressing tumor-bearing mice, we suggest that the effects from systemic administration of CNO are due to ACC inhibition.

The most important contribution of our study is the identification of a contribution of ACC excitatory neurons in mechanical hypersensitivity regulation. We took advantage of optogenetic and chemogenetic approaches to selectively regulate ACC excitatory neurons under the control of CaMKIIα promoter. Compared with traditional excitotoxic lesion and pharmacologic intervention techniques, optogenetic and chemogentic approaches have advantage of greater spatiotemporal specificity and the ability to regulate a larger and specific population of neurons. Our observation that mechanical hypersensivity was reduced by silencing ACC excitatory neurons is consistent with previous pharmacologic intervention studies.[14,39] However, our experiments do not rule out the possible role of ACC interneurons in the regulation of mechanical hypersensitivity. A loss in synaptic inhibition onto excitatory pyramidal neurons in the ACC has been implicated in the development of nerve injury–induced mechanical hypersensivity.[43] Furthermore, it has been recently demonstrated that optogenetic activation of ACC γ-aminobutyric acid–mediated interneurons led to decreased activity of the ACC and reduced nociceptive responses to formalin.[31] These data reinforce the importance of the ACC in mechanical hypersensivity. Put our data into this context, increased ACC activity directly or indirectly through disinhibition of neural network can be speculated to account for the persistence of mechanical hypersensivity.

A pressing question that follows these observations is how the ACC regulates mechanical sensitivity. Although the precise nociceptive circuitry, which allows the ACC to signal to the dorsal horn of the spinal cord to regulate mechanical sensitivity, has not yet been established, two potential corticospinal pathways may be involved. Central nociception regulation can be achieved through descending modulation of the dorsal horn of the spinal cord *via* the periaqueductal gray–rostral ventromedial medulla pathway.[44] Considering the ACC sends projections to the periaqueductal gray,[45] it raises the possibility that the ACC may use this descending modulatory pathway to regulate mechanical sensitivity. This possibility is supported by a previous study that reported that stimulation of the ACC of adult rats facilitated spinal nociceptive tail-flick reflex by acting through brainstem descending modulation

systems.[46] Furthermore, using both the anterograde and retrograde tracing techniques, a recent study has shown that neurons in the deep layers of ACC send direct descending projections to the dorsal horn of the spinal cord in adult mice.[30] It is plausible that the ACC can also use this top-down corticospinal projection to regulate mechanical sensitivity. In the current study, we confirm the existence of a direct corticospinal projection from the ACC to the spinal cord dorsal horn. This finding is also consistent with previous reports from rats and monkeys showing that some of ACC neurons send their axons to the spinal cord.[47,48] However, at this point, due to technical limitation in optically stimulating the ChR2-infected axon terminals in the spinal cord in conscious freely moving animals, our study does not definitively confirm whether ACC contributes to maintain mechanical hypersensitivity relying on its direct, polysynaptic indirect, or both descending inputs to the dorsal horn of the spinal cord. Considering that glutamate is the major excitatory neurotransmitter for ACC projecting neurons, it raises the possibility that glutamate may act as a transmitter for facilitating nociceptive transmission in the spinal cord.[30]

In conclusion, our data suggest that tumor-induced injury or remodeling of primary afferent sensory nerve fibers that innervate the tumor-bearing bone may cause a persistent increase in ACC excitatory neuronal activity, resulting in enhancing nociceptive transmission in the spinal cord, eventually leading to mechanical hypersensitivity. Inhibition of ACC excitatory neuronal activity can potentially reduce bone cancer–induced mechanical hypersensitivity. Our findings highlight the functional importance of the ACC in the maintenance of chronic pain–related behaviors.

Research Support

Supported by research grants from the National Health Research Institute, Zhunan, Taiwan (NHRI-EX104-10336NI); the Ministry of Science and Technology, Taipei, Taiwan (MOST 104-2321-B-006-007); and the Ministry of Education (Aim for the Top University Project to the National Cheng Kung University), Taipei, Taiwan.

Competing Interests

The authors declare no competing interests.

Correspondence

Address correspondence to Dr. Hsu: Department of Pharmacology, College of Medicine, National Cheng Kung University, No. 1, University Rd., Tainan City 701, Taiwan. richard@mail.ncku.edu.tw. Information on purchasing reprints may be found at www.anesthesiology.org or on the masthead page at the beginning of this issue. Anesthesiology's articles are made freely accessible to all readers, for personal use only, 6 months from the cover date of the issue.

References

1. Johansen JP, Fields HL, Manning BH: The affective component of pain in rodents: Direct evidence for a contribution of the anterior cingulate cortex. Proc Natl Acad Sci USA 2001; 98:8077–82
2. Reid KJ, Harker J, Bala MM, Truyers C, Kellen E, Bekkering GE, Kleijnen J: Epidemiology of chronic non-cancer pain in Europe: Narrative review of prevalence, pain treatments and pain impact. Curr Med Res Opin 2011; 27:449–62
3. Descalzi G, Ikegami D, Ushijima T, Nestler EJ, Zachariou V, Narita M: Epigenetic mechanisms of chronic pain. Trends Neurosci 2015; 38:237–46
4. Navratilova E, Porreca F: Reward and motivation in pain and pain relief. Nat Neurosci 2014; 17:1304–12
5. Zhuo M: Cortical excitation and chronic pain. Trends Neurosci 2008; 31:199–207
6. Fuchs PN, Peng YB, Boyette-Davis JA, Uhelski ML: The anterior cingulate cortex and pain processing. Front Integr Neurosci 2014; 8:35
7. Price DD: Psychological and neural mechanisms of the affective dimension of pain. Science 2000; 288:1769–72
8. Cifre I, Sitges C, Fraiman D, Muñoz MÁ, Balenzuela P, González-Roldán A, Martínez-Jauand M, Birbaumer N, Chialvo DR, Montoya P: Disrupted functional connectivity of the pain network in fibromyalgia. Psychosom Med 2012; 74:55–62
9. Peyron R, García-Larrea L, Grégoire MC, Convers P, Richard A, Lavenne F, Barral FG, Mauguière F, Michel D, Laurent B: Parietal and cingulate processes in central pain. A combined positron emission tomography (PET) and functional magnetic resonance imaging (fMRI) study of an unusual case. Pain 2000; 84:77–87
10. Yuan W, Dan L, Netra R, Shaohui M, Chenwang J, Ming Z: A pharmaco-fMRI study on pain networks induced by electrical stimulation after sumatriptan injection. Exp Brain Res 2013; 226:15–24
11. Zhuo M: A synaptic model for pain: Long-term potentiation in the anterior cingulate cortex. Mol Cells 2007; 23:259–71
12. Xu H, Wu LJ, Wang H, Zhang X, Vadakkan KI, Kim SS, Steenland HW, Zhuo M: Presynaptic and postsynaptic amplifications of neuropathic pain in the anterior cingulate cortex. J Neurosci 2008; 28:7445–53
13. Bie B, Brown DL, Naguib M: Increased synaptic GluR1 subunits in the anterior cingulate cortex of rats with peripheral inflammation. Eur J Pharmacol 2011; 653:26–31
14. Li XY, Ko HG, Chen T, Descalzi G, Koga K, Wang H, Kim SS, Shang Y, Kwak C, Park SW, Shim J, Lee K, Collingridge GL, Kaang BK, Zhuo M: Alleviating neuropathic pain hypersensitivity by inhibiting PKMzeta in the anterior cingulate cortex. Science 2010; 330:1400–4
15. Chiou CS, Huang CC, Liang YC, Tsai YC, Hsu KS: Impairment of long-term depression in the anterior cingulate cortex of mice with bone cancer pain. Pain 2012; 153:2097–108
16. Clohisy DR, Mantyh PW: Bone cancer pain. Clin Orthop Relat Res 2003; 415(suppl):S279–88
17. Goblirsch MJ, Zwolak PP, Clohisy DR: Biology of bone cancer pain. Clin Cancer Res 2006; 12(20 pt 2):6231s–5s
18. Ballantine HT Jr, Cassidy WL, Flanagan NB, Marino R Jr: Stereotaxic anterior cingulotomy for neuropsychiatric illness and intractable pain. J Neurosurg 1967; 26:488–95
19. Pereira EA, Paranathala M, Hyam JA, Green AL, Aziz TZ: Anterior cingulotomy improves malignant mesothelioma pain and dyspnoea. Br J Neurosurg 2014; 28:471–4
20. Curto-Reyes V, Llames S, Hidalgo A, Menéndez L, Baamonde A: Spinal and peripheral analgesic effects of the CB2 cannabinoid receptor agonist AM1241 in two models of bone cancer-induced pain. Br J Pharmacol 2010; 160:561–73
21. Chaplan SR, Bach FW, Pogrel JW, Chung JM, Yaksh TL: Quantitative assessment of tactile allodynia in the rat paw. J Neurosci Methods 1994; 53:55–63

22. Iyer SM, Montgomery KL, Towne C, Lee SY, Ramakrishnan C, Deisseroth K, Delp SL: Virally mediated optogenetic excitation and inhibition of pain in freely moving nontransgenic mice. Nat Biotechnol 2014; 32:274–8
23. King T, Vardanyan A, Majuta L, Melemedjian O, Nagle R, Cress AE, Vanderah TW, Lai J, Porreca F: Morphine treatment accelerates sarcoma-induced bone pain, bone loss, and spontaneous fracture in a murine model of bone cancer. Pain 2007; 132:154–68
24. Franklin K, Paxinos G: The Mouse Brain in Stereotaxic Coordinates, 3rd edition. San Diego, Elsevier Academic Press, 2008.
25. Amat J, Baratta MV, Paul E, Bland ST, Watkins LR, Maier SF: Medial prefrontal cortex determines how stressor controllability affects behavior and dorsal raphe nucleus. Nat Neurosci 2005; 8:365–71
26. Stachniak TJ, Ghosh A, Sternson SM: Chemogenetic synaptic silencing of neural circuits localizes a hypothalamus→midbrain pathway for feeding behavior. Neuron 2014; 82:797–808
27. Grünewald A, Lax NZ, Rocha MC, Reeve AK, Hepplewhite PD, Rygiel KA, Taylor RW, Turnbull DM: Quantitative quadruple-label immunofluorescence of mitochondrial and cytoplasmic proteins in single neurons from human midbrain tissue. J Neurosci Methods 2014; 232:143–9
28. Liu XB, Jones EG: Localization of alpha type II calcium calmodulin-dependent protein kinase at glutamatergic but not gamma-aminobutyric acid (GABAergic) synapses in thalamus and cerebral cortex. Proc Natl Acad Sci USA 1996; 93:7332–6
29. Armbruster BN, Li X, Pausch MH, Herlitze S, Roth BL: Evolving the lock to fit the key to create a family of G protein-coupled receptors potently activated by an inert ligand. Proc Natl Acad Sci USA 2007; 104:5163–8
30. Chen T, Koga K, Descalzi G, Qiu S, Wang J, Zhang LS, Zhang ZJ, He XB, Qin X, Xu FQ, Hu J, Wei F, Huganir RL, Li YQ, Zhuo M: Postsynaptic potentiation of corticospinal projecting neurons in the anterior cingulate cortex after nerve injury. Mol Pain 2014; 10:33
31. Gu L, Uhelski ML, Anand S, Romero-Ortega M, Kim YT, Fuchs PN, Mohanty SK: Pain inhibition by optogenetic activation of specific anterior cingulate cortical neurons. PLoS One 2015; 10:e0117746
32. Rainville P, Duncan GH, Price DD, Carrier B, Bushnell MC: Pain affect encoded in human anterior cingulate but not somatosensory cortex. Science 1997; 277:968–71
33. Rainville P, Carrier B, Hofbauer RK, Bushnell MC, Duncan GH: Dissociation of sensory and affective dimensions of pain using hypnotic modulation. Pain 1999; 82:159–71
34. Treede RD, Kenshalo DR, Gracely RH, Jones AK: The cortical representation of pain. Pain 1999; 79:105–11
35. Gao YJ, Ren WH, Zhang YQ, Zhao ZQ: Contributions of the anterior cingulate cortex and amygdala to pain- and fear-conditioned place avoidance in rats. Pain 2004; 110:343–53
36. Johannes CB, Le TK, Zhou X, Johnston JA, Dworkin RH: The prevalence of chronic pain in United States adults: Results of an Internet-based survey. J Pain 2010; 11:1230–9
37. LaGraize SC, Fuchs PN: GABAA but not GABAB receptors in the rostral anterior cingulate cortex selectively modulate pain-induced escape/avoidance behavior. Exp Neurol 2007; 204:182–94
38. Barthas F, Sellmeijer J, Hugel S, Waltisperger E, Barrot M, Yalcin I: The anterior cingulate cortex is a critical hub for pain-induced depression. Biol Psychiatry 2015; 77:236–45
39. Wu LJ, Toyoda H, Zhao MG, Lee YS, Tang J, Ko SW, Jia YH, Shum FW, Zerbinatti CV, Bu G, Wei F, Xu TL, Muglia LJ, Chen ZF, Auberson YP, Kaang BK, Zhuo M: Upregulation of forebrain NMDA NR2B receptors contributes to behavioral sensitization after inflammation. J Neurosci 2005; 25:11107–16
40. Donahue RR, LaGraize SC, Fuchs PN: Electrolytic lesion of the anterior cingulate cortex decreases inflammatory, but not neuropathic nociceptive behavior in rats. Brain Res 2001; 897:131–8
41. Davis KD, Hutchison WD, Lozano AM, Dostrovsky JO: Altered pain and temperature perception following cingulotomy and capsulotomy in a patient with schizoaffective disorder. Pain 1994; 59:189–99
42. Lee GH, Kim SS: Therapeutic strategies for neuropathic pain: Potential application of pharmacosynthetics and optogenetics. Mediators Inflamm 2016; 2016:5808215
43. Blom SM, Pfister JP, Santello M, Senn W, Nevian T: Nerve injury-induced neuropathic pain causes disinhibition of the anterior cingulate cortex. J Neurosci 2014; 34:5754–64
44. Morgan MM, Sohn JH, Liebeskind JC: Stimulation of the periaqueductal gray matter inhibits nociception at the supraspinal as well as spinal level. Brain Res 1989; 502:61–6
45. Floyd NS, Price JL, Ferry AT, Keay KA, Bandler R: Orbitomedial prefrontal cortical projections to distinct longitudinal columns of the periaqueductal gray in the rat. J Comp Neurol 2000; 422:556–78
46. Calejesan AA, Kim SJ, Zhuo M: Descending facilitatory modulation of a behavioral nociceptive response by stimulation in the adult rat anterior cingulate cortex. Eur J Pain 2000; 4:83–96
47. Galea MP, Darian-Smith I: Multiple corticospinal neuron populations in the macaque monkey are specified by their unique cortical origins, spinal terminations, and connections. Cereb Cortex 1994; 4:166–94
48. Gabbott PL, Warner TA, Jays PR, Salway P, Busby SJ: Prefrontal cortex in the rat: Projections to subcortical autonomic, motor, and limbic centers. J Comp Neurol 2005; 492:145–77